



**HAL**  
open science

# First-principle based modeling of urea decomposition kinetics in aqueous solutions

André Nicolle, Stefania Cagnina, Theodorus de Bruin

► **To cite this version:**

André Nicolle, Stefania Cagnina, Theodorus de Bruin. First-principle based modeling of urea decomposition kinetics in aqueous solutions. *Chemical Physics Letters*, 2016, 664, pp.149-153. 10.1016/j.cplett.2016.10.032 . hal-01449373

**HAL Id: hal-01449373**

**<https://hal.science/hal-01449373>**

Submitted on 30 Jan 2017

**HAL** is a multi-disciplinary open access archive for the deposit and dissemination of scientific research documents, whether they are published or not. The documents may come from teaching and research institutions in France or abroad, or from public or private research centers.

L'archive ouverte pluridisciplinaire **HAL**, est destinée au dépôt et à la diffusion de documents scientifiques de niveau recherche, publiés ou non, émanant des établissements d'enseignement et de recherche français ou étrangers, des laboratoires publics ou privés.

# 1 First-principle Based Modeling of Urea Decomposition

## 2 Kinetics in Aqueous Solutions

3 André Nicolle<sup>1,\*</sup>, Stefania Cagnina<sup>1</sup>, Theodorus de Bruin<sup>2</sup>

4 <sup>1</sup> Powertrain and Vehicle Division, IFP Energies Nouvelles, 1 et 4 avenue de Bois-Préau,  
5 92852 Rueil-Malmaison Cedex, France; Institut Carnot IFPEN Transports Energie, France

6 <sup>2</sup> Applied Chemistry and Physical Chemistry Division, IFP Energies Nouvelles, 1 et 4 avenue  
7 de Bois-Préau, 92852 Rueil-Malmaison Cedex, France

8 \* Corresponding author : andre.nicolle@ifpen.fr, Phone : +33 1 47 52 66 88

### 9 **Keywords**

10 Urea, decomposition, multiscale modeling, kinetics, *ab initio*, *water cooperation*

### 11 **Abstract**

12 This study aims at validating a multi-scale modeling methodology based on an implicit  
13 solvent model for urea thermal decomposition pathways in aqueous solutions. The influence  
14 of the number of cooperative water molecules on kinetics was highlighted. The obtained  
15 kinetic model is able to accurately reproduce urea decomposition in aqueous phase under a  
16 variety of experimental conditions from different research groups. The model also highlights  
17 the competition between HNCO desorption to gas phase and hydrolysis in aqueous phase,  
18 which may influence SCR depollution process operation.

## 21 1. Introduction

22 Urea decomposition kinetics is important for a vast variety of applications, including  
23 agriculture [1], medical technologies [2] and energy [3]. In lean-burn automotive exhaust  
24 aftertreatment systems, a urea-water solution is injected upstream of the deNO<sub>x</sub> catalyst to  
25 generate ammonia for the selective catalytic reduction (SCR) process. Previous studies  
26 showed that urea aqueous phase decomposition can compete effectively with water  
27 evaporation rate [4] and urea polymerization [5]. While a number of recent studies [6] [7]  
28 contributed to the elucidation of main urea decomposition pathways in aqueous solution, the  
29 mechanism of ammonia and isocyanic acid release remains insufficiently understood,  
30 although a molecular mechanism for the homolytic breaking of C-N bond seems more  
31 plausible than an ionic one [8]. Among the homolytic decomposition channels identified  
32 (ammonia elimination, hydrolysis and tautomerization), Alexandrova and Jorgensen [6] found  
33 the first path to have the lowest activation energy, partly resulting from the resonance  
34 stabilization in the first transition state. However, their study mainly focused on the solvent  
35 effects on the potential energy surface (PES), but not on the corresponding kinetic rate  
36 constants. These authors did not investigate the subsequent hydrolysis of isocyanic acid  
37 leading to an additional ammonia production. In the present study, we demonstrated the  
38 feasibility of a multiscale first-principle based kinetic modeling of urea decomposition in  
39 aqueous solution. We performed a high-level electronic structure study on the main ammonia  
40 production paths from urea decomposition including an implicit solvent model. Based on  
41 these new results, we herein derived the corresponding phenomenological rate constants and  
42 thermokinetic data to build a macrokinetic mechanism, which was subsequently validated  
43 against experimental data, allowing rate-of-production studies of urea decomposition under  
44 realistic operating conditions.

45

## 46 2. Methodology

1  
2  
3 47 The electronic structure calculations were performed with the Gaussian 09 suite of programs  
4  
5 48 [9]. All geometry optimizations were performed at the M06-2X/6-311++G(d,p) level of  
6  
7  
8 49 theory to correctly describe long-range hydrogen bonding [10]. Systematic conformational  
9  
10 50 searches were performed to identify the most stable structures. The T1 diagnostic for all  
11  
12  
13 51 species involved in this work was less than 0.02, supporting the appropriateness of single-  
14  
15 52 reference methods in describing the wave function. Frequency calculations confirmed the  
16  
17  
18 53 desired character of the stationary points and IRC calculations effectively ensured the  
19  
20 54 connection between the reactants and products. In DFT calculations, we used the SMD  
21  
22 55 implicit solvent model [11], which is known to produce errors for solvation energies typically  
23  
24  
25 56 lower than 1 kcal/mol for neutral molecules. Post Hartree-Fock energies were determined for  
26  
27 57 the most important reaction steps by performing CCSD(T)/aug-cc-pVTZ evaluations using  
28  
29  
30 58 Molpro 2015 program [12] on the geometries previously optimized at the DFT level. The  
31  
32 59 ZPE-corrected Gibbs free energy was evaluated using the following formula:

$$35 \quad G = E(\text{CCSD}(T)//\text{DFT}) + G_{\text{corr}}(\text{DFT}) + \Delta E_{\text{solvation,DFT,0K}}$$

36  
37  
38  
39 61 In this equation  $E$  refers to the electronic energy and  $G_{\text{corr}}$  to the thermal corrections to the  
40  
41 62 Gibbs Free energy, which envelopes the ZPE correction together with the translational,  
42  
43  
44 63 rotational and vibrational enthalpic and entropic corrections, calculated using M06-2X at the  
45  
46  
47 64 desired pressure and temperature.  $\Delta E_{\text{solvation}}$  corresponds to the gas-to-water solvation energy,  
48  
49 65 calculated at the M06-2X level without any thermal correction.

50  
51  
52 66 The harmonic transition state theory was selected to compute the corresponding  
53  
54  
55 67 phenomenological rate constants. Wigner correction factors [13] were computed to account  
56  
57  
58 68 for tunneling effects. Free activation energies were computed over the 300-600 K temperature  
59  
60 69 range to get phenomenological rate constants in the Arrhenius-Kooij form  
61  
62  
63  
64  
65

1  
2  
3  
4  
5  
6  
7  
8  
9  
10  
11  
12  
13  
14  
15  
16  
17  
18  
19  
20  
21  
22  
23  
24  
25  
26  
27  
28  
29  
30  
31  
32  
33  
34  
35  
36  
37  
38  
39  
40  
41  
42  
43  
44  
45  
46  
47  
48  
49  
50  
51  
52  
53  
54  
55  
56  
57  
58  
59  
60  
61  
62  
63  
64  
65

70  $k = A \left( \frac{T}{1\text{ K}} \right)^n \exp \left( - \frac{E}{RT} \right)$ . Macrokinetic modeling was carried out using the homogeneous  
71 (CSTR) reactor model implemented in Chemkin software package [14]. The same condensed-  
72 phase mean-field macrokinetic formalism was used as in our previous work [4]. The reverse  
73 rate constants were computed from the corresponding forward ones and reaction Gibbs free  
74 energies. The Weizmann-1 (W1) theory [15] was used to determine the enthalpies of the  
75 energetic minima of the PES over the 300-600 K range and the obtained thermochemical data  
76 were implemented in the mechanism using the NASA formalism [16]. As can be seen in  
77 Table S1 (supplementary material), W1 theory coupled to SMD solvation model accurately  
78 predicts the available experimental thermochemical data, demonstrating its suitability for the  
79 present bottom-up kinetic modeling approach. Desorption rates were modeled from  
80 recommended [17] sticking coefficients (0.1 for NH<sub>3</sub>, HNCO and CO<sub>2</sub>) using Hertz-Knudsen  
81 equation and equilibrium constants evaluated from thermochemical data.

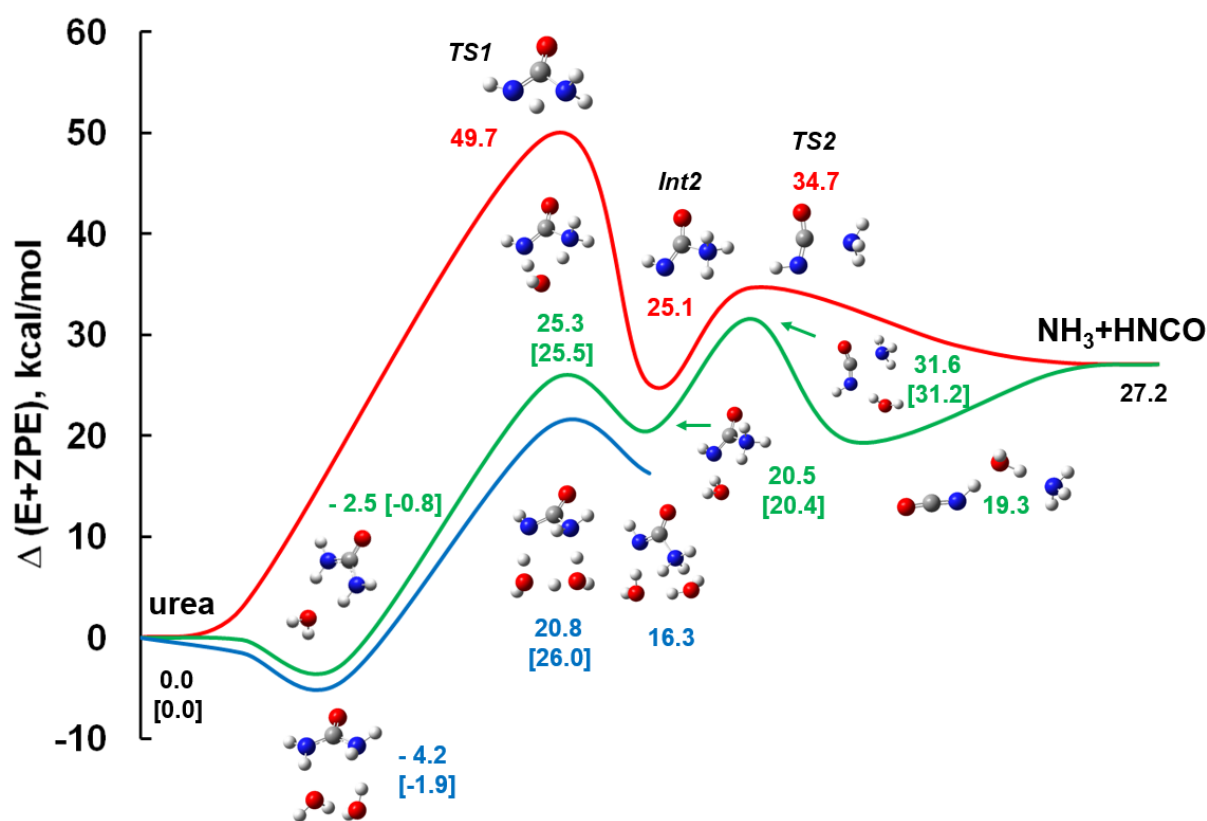
### 82 83 **3. Results and discussion**

84 Our electronic structure calculations confirm, referring to the work of Jorgensen [6], that  
85 water-assisted NH<sub>3</sub> elimination has a lower free energy of activation than hydrolysis (Figure  
86 S1 in supplementary material). As shown in Table 1, the Gibbs free energy barriers at 300 K  
87 and 1 atm for NH<sub>3</sub>CONH (Int 2) formation through water-assisted H-shuttling lie at 30.9 and  
88 30.3 kcal/mol for respectively one and two H<sub>2</sub>O molecules involved, in good agreement with  
89 the values obtained by Tsipis [23], Alexandrova [6] and Yao [7] (respectively 29.5, 26.4 and  
90 25.3 kcal/mol). The Free energy barrier associated to nucleophilic attack of water on carbonyl  
91 is much higher than this value, favoring NH<sub>3</sub> elimination over urea hydrolysis. It is important  
92 to note that relative DFT energies can differ from post-HF values by up to 10 kcal/mol

93 (Figure 2), which highlights the importance of a fine description of the electron correlation to  
 94 get accurate energetic barriers.

Urea + H <sub>2</sub> O → NH <sub>3</sub> +HNCO+H <sub>2</sub> O				Urea + 2 H <sub>2</sub> O → NH <sub>3</sub> +HNCO+2 H <sub>2</sub> O		HNCO + H <sub>2</sub> O + NH <sub>3</sub> → NH <sub>2</sub> COOH + NH <sub>3</sub>		HNCO + 2 H <sub>2</sub> O → NH <sub>2</sub> COOH + H <sub>2</sub> O	
complex	TS1	Int2	TS2	complex	TS1	complex	TS3	complex	TS3
4.1	35.0	28.2	38.2	14.5	44.8	11.0	30.6	12.2	36.0

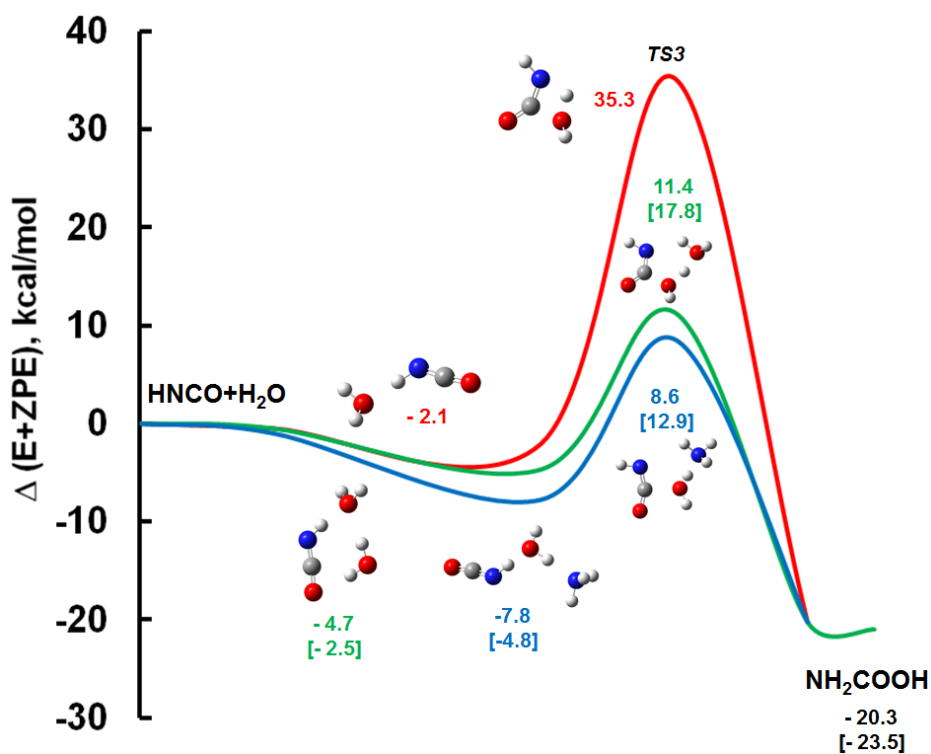
96 Table 1 – Relative Gibbs Free energies at 300 K and 1 atm with respect to the reactants



97  
 98 Figure 1 - Relative ZPE-corrected electronic energies (in kcal/mol) obtained at the M06-2X and  
 99 CCSD(T)/M06-2X levels (in brackets) for unimolecular and water-assisted NH<sub>3</sub> elimination. Red, green and  
 100 blue curves correspond respectively to zero, one and two assisting water molecules. Since the energy potential  
 101 for C-N bond fission is weakly dependent on water involvement, this step was not studied in presence of 2 H<sub>2</sub>O  
 102 molecules.

104 The subsequent hydrolysis of HNCO (Figure 2) proceeds through the formation of carbamic  
105 acid, which can in turn decompose through either intramolecular or assisted mechanism. In  
106 the present study, we focused on the addition of water across the C=N bond of HNCO, as it is  
107 energetically more favorable [24] than addition across the C=O bond due to the extended  
108 concentration of the electron density on nitrogen [25]. Although a competitive bicarbonate  
109 mechanism could also be considered in this study, it is not expected to change HNCO  
110 hydrolysis kinetics since the transition state (TS) structures involved are very similar [26]. As  
111 could be anticipated [27], the six-membered-ring TS involving two water molecules results in  
112 a lower barrier (19.7 kcal/mol) compared to a four-membered-ring TS (38.9 kcal/mol).  
113 According to Wei et al. [24], the former barrier lies less than 4 kcal/mol from the value  
114 obtained by considering an eight-membered cyclic TS, showing the fast convergence of this  
115 barrier with the number of water molecules. Interestingly, water addition assisted by ammonia  
116 (instead of water) shows a significantly lower energetic barrier.

117



118

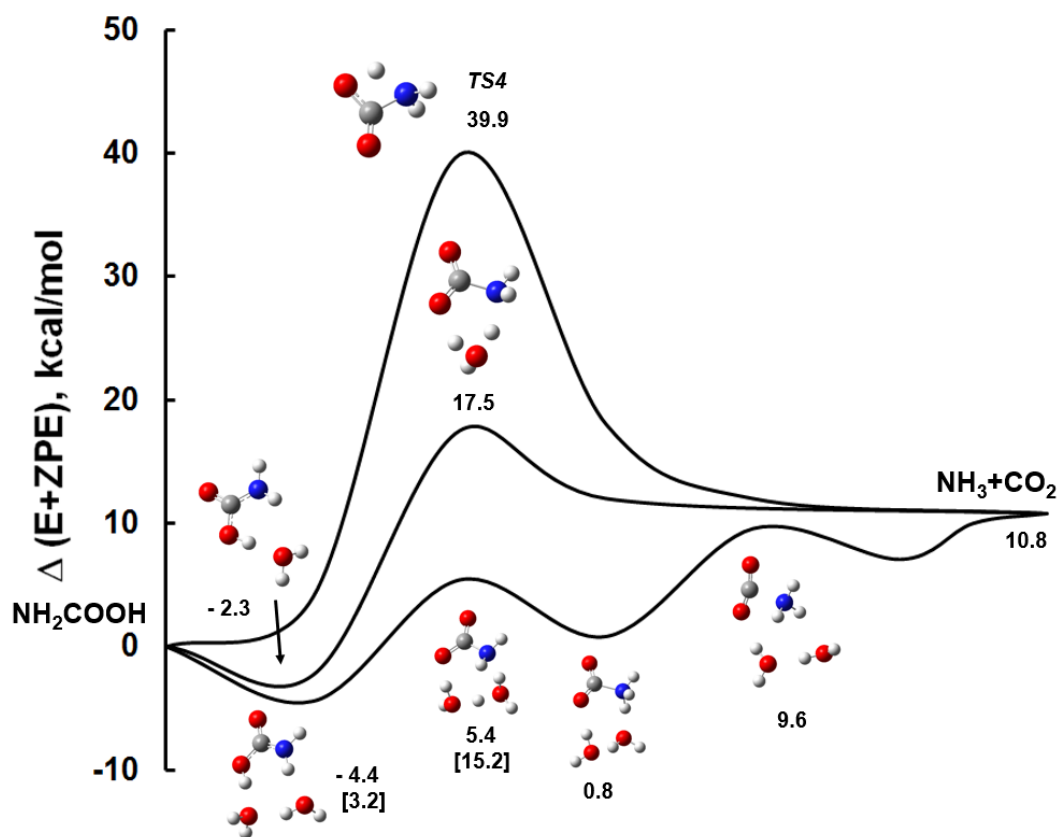
119

120

121

122

Figure 2 - Relative ZPE-corrected electronic energies (in kcal/mol) obtained at the M06-2X and CCSD(T)/M06-2X levels (in brackets) for HNC(O) hydrolysis. Red, green and blue curves correspond respectively to zero, one water and one ammonia assisting molecules.



122

123

124

Figure 3 - Relative ZPE-corrected electronic energies (in kcal/mol) obtained at the M06-2X and CCSD(T)/M06-2X levels (in brackets) for NH<sub>3</sub> elimination from carbamic acid.



1  
2 126 As can be seen on Figure 3, the energetic barriers for carbamic acid decarboxylation are also  
3  
4 127 highly dependent on the number of water molecules involved. As for HNCO, the attack of one  
5  
6  
7 128 water molecule on C=N bond (barrier of 19.8 kcal/mol) is more favorable than an attack of  
8  
9 129 water on C=O bond (barrier of 27.5 kcal/mol reported in [28]). The geometry of the six-  
10  
11 130 membered cyclic TS (obtained by considering one water molecule) is globally similar to the  
12  
13 131 gas-phase TS described by Tsipis et al. [29], although water's oxygen lies clearly out-of-plane  
14  
15 132 (respective OCNO dihedral angles of  $7.2^\circ$  and  $32.0^\circ$ ). Note also that this H-shuttling  
16  
17 133 mechanism is similar to that reported by Ramachandran [30] for ammonia-assisted  
18  
19 134 decomposition of carbamic acid in dry medium, who obtained a Free energy barrier of 18  
20  
21 135 kcal/mol, in contrast with Cheng et al. [31] who considered a four-membered ring TS  
22  
23 136 structure, thereby leading to a barrier similar to that of the unassisted decarboxylation. As the  
24  
25 137 number of water molecules increases, an additional local minimum appears in the energetic  
26  
27 138 potential. The energetic barrier obtained in the case of the assistance of two water molecules  
28  
29 139 (12.0 kcal/mol) is significantly lower than the reported value of 15.0 kcal/mol previously  
30  
31 140 obtained at a lower level of theory (with only one water molecule) by Ruelle et al. [32] and  
32  
33 141 the experimental value (15.6 kcal/mol) reported by Wang et al. [33] However, it is in good  
34  
35 142 agreement with the barrier of 10.3 kcal/mol recently claimed by Noble et al. [34] in the  
36  
37 143 presence of 6 H<sub>2</sub>O molecules.  
38  
39  
40  
41  
42  
43  
44  
45  
46  
47  
48  
49  
50  
51  
52  
53  
54  
55  
56  
57  
58  
59  
60  
61  
62  
63  
64  
65

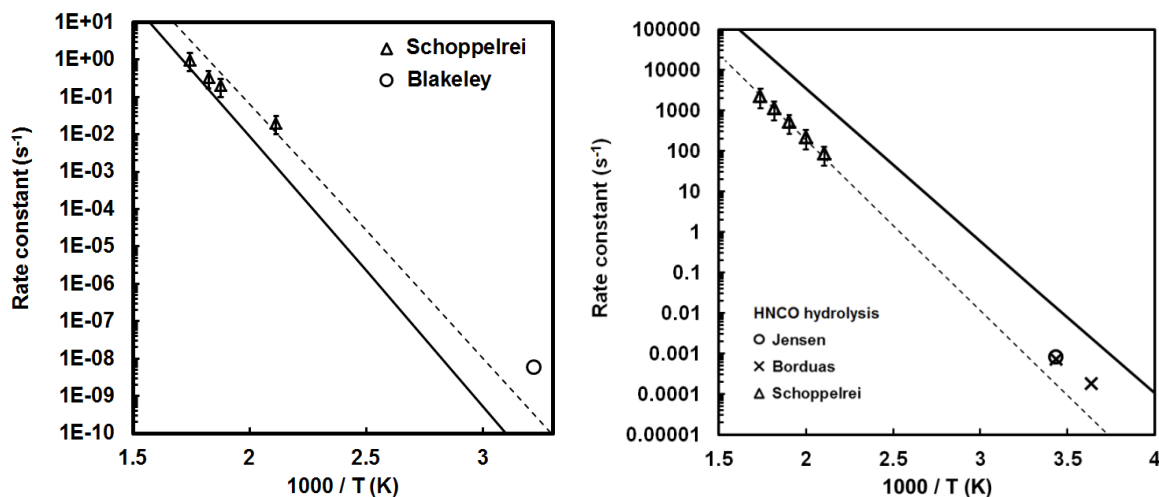
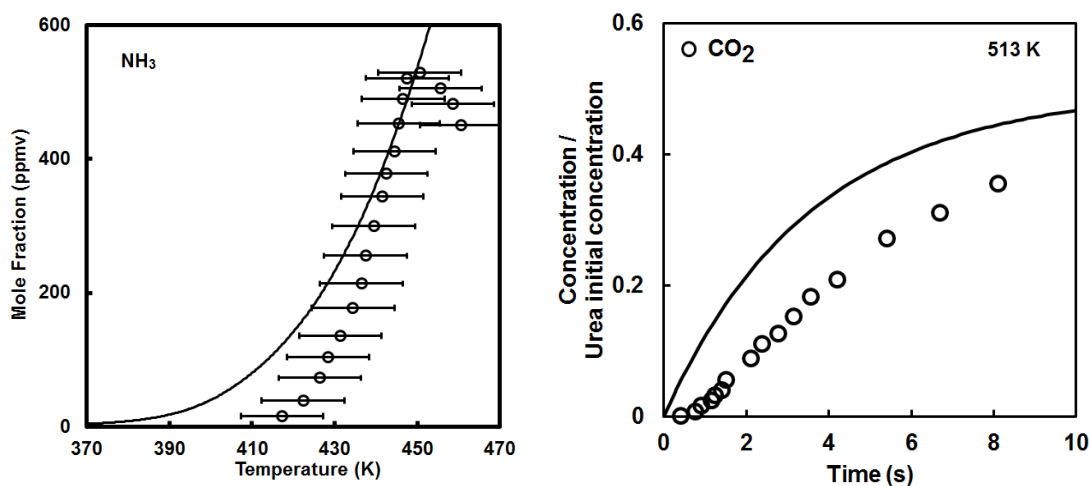


Figure 4 - Calculated and measured [35] [20] [36] [37] [38] rate constants for ammonia elimination from urea (left) and HNCO hydrolysis (right) in water solution. For  $\text{NH}_3$  elimination, the quasi-steady state approximation (QSS) on Int2 ( $\text{NH}_3\text{CONH}$ ) is applied (see text). The dotted line on the left denotes the ab initio rate constant with an activation energy decreased by 2 kcal/mol. The dotted line on the right corresponds to the ab initio rate constant including Kramers barrier recrossing correction and with an activation energy increased by 2 kcal/mol.

Rate constant calculations for the most favorable reaction pathways were subsequently performed to derive phenomenological rate constants from the multi-well free energy surface. Arrhenius-Kooij least-squares fits on calculated rate constant values for most favorable water-assisted channels are provided in Table S2 (supplementary material). As can be noticed from the comparison with experimental data in Figure 4, within the uncertainties on molecular parameters, the present multi-scale approach is able to generate accurate rate coefficients (within a factor of 2) over an extended temperature range. Note that the rate constants of backward reaction  $\text{Int2} \rightarrow \text{Urea}$  ( $3.08 \times 10^9 \text{ s}^{-1}$  at 500 K) and second step  $\text{Int2} \rightarrow \text{NH}_3 + \text{HNCO}$  ( $1.54 \times 10^9 \text{ s}^{-1}$  at 500 K) remain much higher than forward reaction  $\text{Urea} \rightarrow \text{Int2}$  ( $2.04 \times 10^{-02} \text{ s}^{-1}$  at 500 K) over a wide range of temperatures, therefore Int2 ( $\text{NH}_3\text{CONH}$ ) can be assumed to be in quasi steady state (QSS). Under these conditions, our calculations indicate

163 that the rate-limiting step switches between  $\text{Int2} \rightarrow \text{NH}_3 + \text{HNCO}$  at  $T < 600 \text{ K}$  and  $\text{Urea} \rightarrow$   
164  $\text{Int2}$  at  $T > 600 \text{ K}$  [39]. It is also worth noting that except for very high urea concentrations in  
165 water solution ( $> 10 \text{ M}$ ), intrinsic reaction kinetics is not expected to be limited by cage  
166 diffusion ( $4\pi\sigma D_{\text{urea/water}} N_A C_{\text{urea}} \sim 10^{10} \text{ s}^{-1}$ ) at temperatures of interest ( $T < 1000 \text{ K}$ ) [40].

167  
168 Even though the rate constant is mostly sensitive to the TS1 relative electronic energy (Figure  
169 S2 in supplementary material), the sensitivity to vibrational and rotational partition functions  
170 of TS1 (respectively through frequencies and moments of inertia) is significant. As the error  
171 on the herein obtained vibrational frequencies is typically of the order of a few percent and  
172 since anharmonicity is not accounted for in this study, a significant uncertainty ( $> 10\%$ )  
173 remains on the partition function.



175  
176 *Figure 5 – On the left, calculated (lines) and measured (symbols) species gas-phase  $\text{NH}_3$  mole fraction, where*  
177 *the experimental uncertainty was deduced from reproducibility tests carried out by the authors[41]. On the*  
178 *right, the  $\text{CO}_2$  liquid-phase mole fraction profiles during urea-water solution decomposition. [37]*

180 Figure 5 shows ammonia concentration profiles obtained using the *ab initio* kinetic model  
181 (Table S2, supplementary material). This model reproduces well the onset of NH<sub>3</sub> release, but  
182 it tends to overestimate the ammonia concentration at temperatures higher than 470 K. This  
183 can be attributed to the concurrent formation of biuret (NH<sub>2</sub>C(O)NHC(O)NH<sub>2</sub>) from urea and  
184 HNCO, which is not accounted for by the present kinetic model. In Lundström's experimental  
185 conditions [41], our reaction flux analyses at 400 K indicate that HNCO hydrolysis rate in  
186 aqueous phase contributes to 35% of HNCO consumption while HNCO desorption to gas  
187 phase represents 65% of its consumption. Therefore, according to this model, HNCO  
188 hydrolysis is expected to contribute significantly to NH<sub>3</sub> production in SCR process  
189 conditions.

190 Note that urea selectivity to CO<sub>2</sub> formation is also well predicted by the present *ab initio*  
191 kinetic model (Figure 5). Further, the present model predicts that the carbamic acid maximum  
192 mole fraction in aqueous solution should be of the order of 1 ppm under urea decomposition  
193 conditions, calling for quantitative measurements of this intermediate. Due to the high Free  
194 energy barrier involved, the contribution of urea hydrolysis should remain negligible under  
195 the investigated conditions, although it can be anticipated [4] [42] that higher heating rates  
196 would shift NH<sub>3</sub> conversion profile towards higher temperatures, thereby favoring direct urea  
197 hydrolysis.

#### 198 **4. Conclusions**

199 A multi-scale modeling methodology based on electronic structure calculations using an  
200 implicit solvent model, transition state theory and macrokinetic modeling was validated on the  
201 important issue of homolytic urea thermal decomposition in aqueous solutions. The influence  
202 of the number of cooperative water molecules on reaction kinetics was highlighted. The  
203 obtained macrokinetic model is able to reproduce urea decomposition in the aqueous phase

204 under a variety of experimental conditions from different groups. The evidence of occurrence  
205 of urea decomposition in aqueous solution under typical SCR operating conditions should  
206 encourage engineers to include these hitherto neglected paths in their kinetic models [43].  
207 Notably, the model reveals that HNCO hydrolysis in aqueous phase competes effectively with  
208 its desorption, providing evidence of the contribution of condensed phase HNCO hydrolysis  
209 during SCR process operation. While the present obtained thermokinetic data will allow more  
210 accurate modeling of industrial and biological systems, further work is needed to extend the  
211 model to urea polymerization in aqueous and dry media [44] [45] to get more accurate  
212 predictions of urea decomposition at higher temperatures.

## 213 **Acknowledgments**

214 SC would like to thank IFPEN for a post-doctoral grant. This research did not receive any  
215 other specific grant from funding agencies in the public, commercial or not-for-profit sector.

## 216 **Supporting information**

217 Additional informations including the geometries of the most important stationary points  
218 obtained in the present study are available as a supplementary material.

## 219 **References**

- 220  
221 [1] M.L. Cabrera, D.E. Kissel, B.R. Bock, *Soil Biology and Biochemistry* 23 (1991) 1121.  
222 [2] D. El-Gamal, S.P. Rao, M. Holzer, S. Hallstrom, J. Haybaeck, M. Gauster, C. Wadsack, A. Kozina, S.  
223 Frank, R. Schicho, R. Schuligoi, A. Heinemann, G. Marsche, *Kidney international* 86 (2014) 923.  
224 [3] R. Rota, D. Antos, É.F. Zanoelo, M. Morbidelli, *Chemical Engineering Science* 57 (2002) 27.  
225 [4] V. Ebrahimian, A. Nicolle, C. Habchi, *AIChE Journal* 58 (2012) 1998.  
226 [5] P.M. Schaber, J. Colson, S. Higgins, D. Thielen, B. Anspach, J. Brauer, *Thermochimica Acta* 424 (2004)  
227 131.  
228 [6] A.N. Alexandrova, W.L. Jorgensen, *The Journal of Physical Chemistry. B* 111 (2007) 720.  
229 [7] M. Yao, X. Chen, C.-G. Zhan, *Chemical Physics Letters* 625 (2015) 143.  
230 [8] J. Shorter, *Chemical Society Review* 7 (1978) 1.  
231 [9] M. J. Frisch, G. W. Trucks, H. B. Schlegel, G. E. Scuseria, M. A. Robb, J. R. Cheeseman, G. Scalmani, V.  
232 Barone, B. Mennucci, G. A. Petersson, H. Nakatsuji, M. Caricato, X. Li, H. P. Hratchian, A. F. Izmaylov, J.  
233 Bloino, G. Zheng, J. L. Sonnenberg, M. Hada, M. Ehara, K. Toyota, R. Fukuda, J. Hasegawa, M. Ishida, T.

234 Nakajima, Y. Honda, O. Kitao, H. Nakai, T. Vreven, Montgomery, Jr., J. A., J. E. Peralta, F. Ogliaro, M.  
1 235 Bearpark, J. J. Heyd, E. Brothers, K. N. Kudin, V. N. Staroverov, R. Kobayashi, J. Normand, K.  
2 236 Raghavachari, A. Rendell, J. C. Burant, S. S. Iyengar, J. Tomasi, M. Cossi, N. Rega, J. M. Millam, M.  
3 237 Klene, J. E. Knox, J. B. Cross, V. Bakken, C. Adamo, J. Jaramillo, R. Gomperts, R. E. Stratmann, O.  
4 238 Yazyev, A. J. Austin, R. Cammi, C. Pomelli, J. W. Ochterski, R. L. Martin, K. Morokuma, V. G.  
5 239 Zakrzewski, G. A. Voth, P. Salvador, J. J. Dannenberg, S. Dapprich, A. D. Daniels, Ö. Farkas, J. B.  
6 240 Foresman, J. V. Ortiz, J. Cioslowski, D. J. Fox, Gaussian 09.  
7 241 [10]Y. Zhao, D.G. Truhlar, *Theor Chem Account* 120 (2008) 215.  
8 242 [11]A.V. Marenich, C.J. Cramer, D.G. Truhlar, *The Journal of Physical Chemistry. B* 113 (2009) 6378.  
9 243 [12]H.-J. Werner, P.J. Knowles, G. Knizia, F.R. Manby, M. Schütz, *WIREs Comput Mol Sci* 2 (2012) 242.  
10 244 [13]E. Wigner, *Z Phys Chem B-Chem E* 19 (1932) 203.  
11 245 [14]E. Meeks, H.K. Moffat, J.F. Grcar, R.J. Kee, Sandia National Laboratories Report SAND96-8218 (1996).  
12 246 [15]J.M.L. Martin, G. de Oliveira, *Journal of Chemical Physics*. 111 (1999) 1843.  
13 247 [16]S. Gordon, B.J. McBride, *NASA SP-273* 168 (1971).  
14 248 [17]M. Ammann, R.A. Cox, J.N. Crowley, M.E. Jenkin, A. Mellouki, M.J. Rossi, J. Troe, T.J. Wallington,  
15 249 *Atmospheric Chemistry and Physics*. 13 (2013) 8045.  
16 250 [18]A.V. Kustov, N.L. Smirnova, *Journal of Chemical & Engineering Data*. 55 (2010) 3055.  
17 251 [19]C.E. Vanderzee, D.L. King, *The Journal of Chemical Thermodynamics* 4 (1972) 675.  
18 252 [20]N. Borduas, B. Place, G.R. Wentworth, J.P.D. Abbatt, J.G. Murphy, *Atmospheric Chemistry and Physics*. 16  
19 253 (2016) 703.  
20 254 [21]J.J. Carroll, J.D. Slupsky, A.E. Mather, *Journal of Physical and Chemical Reference Data*. 20 (1991) 1201.  
21 255 [22]M.W. Chase, NIST-JANAF thermochemical tables, American Chemical Society; American Institute of  
22 256 Physics for the National Institute of Standards and Technology, Woodbury, N.Y., 1998.  
23 257 [23]C.A. Tsipis, P.A. Karipidis, *Journal of the American Chemical Society* 125 (2003) 2307.  
24 258 [24]X.-G. Wei, X.-M. Sun, X.-P. Wu, S. Geng, Y. Ren, N.-B. Wong, W.-K. Li, *Journal of Molecular Modeling*  
25 259 17 (2011) 2069.  
26 260 [25]Greet Raspoet, and Minh Tho Nguyen, Michelle McGarraghy, and Anthony Frank Hegarty, *The Journal of*  
27 261 *Organic Chemistry* 63 (1998) 6867.  
28 262 [26]T.R. Prosochkina, E.L. Artem'eva, E.A. Kantor, *Russian Journal of General Chemistry*. 83 (2013) 10.  
29 263 [27]S. Tolosa Arroyo, A. Hidalgo Garcia, J.A. Sanson Martin, *The Journal of Physical Chemistry A*. 113 (2009)  
30 264 1858.  
31 265 [28]D.Y. Kim, H.M. Lee, S.K. Min, Y. Cho, I.-C. Hwang, K. Han, J.Y. Kim, K.S. Kim, *The Journal of Physical*  
32 266 *Chemistry Letters*. 2 (2011) 689.  
33 267 [29]C.A. Tsipis, P.A. Karipidis, *The Journal of Physical Chemistry A*. 109 (2005) 8560.  
34 268 [30]B.R. Ramachandran, A.M. Halpern, E.D. Glendening, *The Journal of Physical Chemistry A* 102 (1998)  
35 269 3934.  
36 270 [31]X. Cheng, Y. Zhao, W. Zhu, Y. Liu, *Journal of Molecular Modeling* 19 (2013) 5037.  
37 271 [32]P. Ruelle, U.W. Kesselring, N.-T. Hô, *Journal of Molecular Structure: THEOCHEM* 124 (1985) 41.  
38 272 [33]X. Wang, W. Conway, D. Fernandes, G. Lawrance, R. Burns, G. Puxty, M. Maeder, *The Journal of Physical*  
39 273 *Chemistry A* 115 (2011) 6405.  
40 274 [34]J.A. Noble, P. Theule, F. Duvernay, G. Danger, T. Chiavassa, P. Ghesquiere, T. Mineva, D. Talbi, *Physical*  
41 275 *Chemistry Chemical Physics : PCCP* 16 (2014) 23604.  
42 276 [35]M.L. Kieke, J.W. Schoppelrei, T.B. Brill, *The Journal of Physical Chemistry*. 100 (1996) 7455.  
43 277 [36]M.B. Jensen, W. Taub, D. Ginsburg, K. Hartiala, S. Veige, E. Diczfalusy, *Acta Chemica Scandinavica*. 12  
44 278 (1958) 1657.  
45 279 [37]J.W. Schoppelrei, M.L. Kieke, X. Wang, M.T. Klein, T.B. Brill, *The Journal of Physical Chemistry*. 100  
46 280 (1996) 14343.  
47 281 [38]R.L. Blakeley, A. Treston, R.K. Andrews, B. Zerner, *Journal of the American Chemical Society* 104 (1982)  
48 282 612.  
49 283 [39]J.R. Murdoch, *Journal of Chemical Education* 58 (1981) 32.  
50  
51  
52  
53  
54  
55  
56  
57  
58  
59  
60  
61  
62  
63  
64  
65

284 [40]L.S. Sorell, A.S. Myerson, *AIChE Journal* 28 (1982) 772.  
1 285 [41]A. Lundström, B. Andersson, L. Olsson, *Chemical Engineering Journal* 150 (2009) 544.  
2 286 [42]S.A. Skarlis, A. Nicolle, D. Berthout, C. Dujardin, P. Granger, *Thermochimica Acta* 584 (2014) 58.  
3 287 [43]F. Birkhold, U. Meingast, P. Wassermann, O. Deutschmann, *Applied Catalysis B: Environmental* 70 (2007)  
4 288 119.  
5 289 [44]W. Brack, B. Heine, F. Birkhold, M. Kruse, G. Schoch, S. Tischer, O. Deutschmann, *Chemical Engineering*  
6 290 *Science* 106 (2014) 1.  
7 291 [45]S. Sebelius, T.T. Le, L.J. Pettersson, H. Lind, *Chemical Engineering Journal* 231 (2013) 220.  
8  
9

10  
11  
12  
13  
14  
15  
16  
17  
18  
19  
20  
21  
22  
23  
24  
25  
26  
27  
28  
29  
30  
31  
32  
33  
34  
35  
36  
37  
38  
39  
40  
41  
42  
43  
44  
45  
46  
47  
48  
49  
50  
51  
52  
53  
54  
55  
56  
57  
58  
59  
60  
61  
62  
63  
64  
65

**Supplementary Materials**

[Click here to download Supplementary Materials: Supp\\_Mat\\_submitted.docx](#)